TRANSIENT RESPONSE OF A MOORED VESSEL INDUCED BY A PASSING SHIP

Liang Li and **Zhi-Ming Yuan,** Department of Naval Architecture, Ocean and Marine Engineering, Glasgow, UK

SUMMARY

A passing ship sets up the wash waves, which are able to propagate a long distance with limited dissipation. The wash waves will induce transient loads on a moored vessel. In the present research, a hybrid model is developed to estimate the transient response of a moored vessel induced by another passing ship far away. The hybrid method is based on the combination of the 3-D Rankine source method and the impulse response theory. The wash waves and the impact loads acting on the moored vessels are addressed using the 3-D Rankine source method. The transient response of the vessel is simulated with the impulse response theory. The transient response is found to increase with the passing ship's speed. In addition, the propagation distance of the wash waves has a limited influence on the transient response due to the dissipation feature of the divergent wash waves.

1 INTRODUCTION

A ship moored in a port is subjected to complicated external loads, which may induce strong motions of the moored ship. When the motions become very large, marine operations must be terminated and the downtime will be consequently increased. For the safety of operation, the motions of a moored ship in a port should be investigated carefully. Apart from the incident sea waves, a passing ship also causes the moored ship to move. Vantorre et al. (2002) carried out model tests to investigate the hydrodynamic interaction between a moored ship and a passing ship during overtaking operation. Li et al. (2018b) investigated the hydrodynamic interactions between two passing ships during the encountering. Both works proved that the moored ship is subject to considerable hydrodynamic loads due to the passing effect induced by the other ship.

Until now, most studies on the passing ship effect focus on the suction effects induced by the 'double-body' flow around the passing vessel. It inherently implies that the free-surface disturbance and the surface wave propagation are not considered. It is probably because the forward speed of the passing ship is not high in most cases. However, nowadays have seen an increasing number of high-speed vessels, in both open sea and restricted waterways. In this circumstance, the wash waves must be considered. Janson et al. (2003) calculated the wash waves using a combine Rankine/Kelvin source method. Jiang et al. (2002) extended the Boussinesq's equation to capture the far-field wash waves. As well-known (van der Molen and Wenneker, 2008), the wash waves produced by an advancing ship with high speed can travel a long distance with little dissipation so that the moored ship will be subjected to substantial wash wave force even if the passing ship is far away as long as the forward speed is high enough. Pinkster (2009) proposed a computation method to examine the suction, the seiche and the wash effects induced by a passing ship. Pinkster and Naaijen (2003) investigated the passing ship effect accounting for the free-surface disturbance. Li et al. (2018a) simulated the transient motions of a moored ship under the joint action of wash waves and sea waves.

In this work, a hybrid numerical model is developed to investigate the transient response of a ship moored in a port when a ship is passing by with high forward speed. The wash waves and their impact loads on the moored ship are simulated with the 3-D boundary element method based on the Rankine Green function. Subsequently, a hydro-mooring coupled analysis is performed in time-domain to investigate the transient response of the ship.

2 HYBRID NUMERICAL MODEL

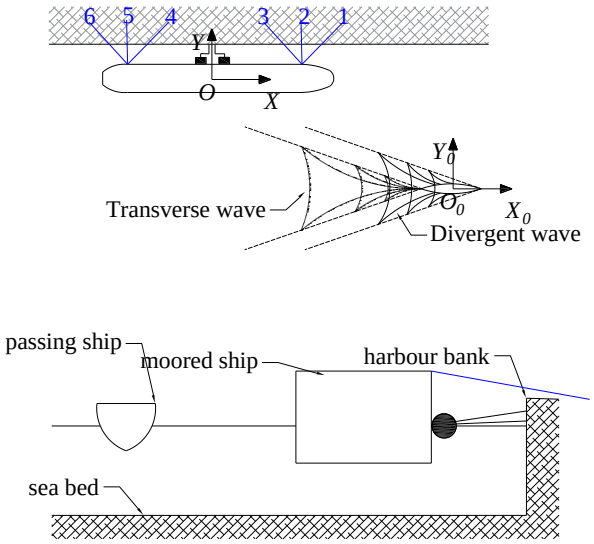

Figure 1. Sketch of a ship passing a ship moored at a port.

The present study is to investigate the transient response of a moored ship in a port subject to the wash waves produced by another passing ship (see Figure 1). The passing ship is a Wigley vessel with the main dimensions listed in

Table 1. It is enforced to travel along positive X direction with a constant forward speed V. The Froude number Fr of the passing ship is 0.8 ($Fr = V / \sqrt{gL_1}$, g is the gravity acceleration). No oscillating motions of the passing ship are allowed. The lateral distance B_S between the two ships is 40 m. The water depth is set to 10 m

Table 1 Main dimensions of the passing ship.

Parameter	Value
Length (L_1)	30 m
Breath (B_1)	6 m
Draft (D_1)	1.875 m

The ship is moored in the port through the hawser-fender system. The gap width between the moored ship and the port bank is 13 m. The main dimensions of the moored ship are listed in Table 2.

Table 2 Main dimensions of the moored ship.

Parameter	Value
Length (L_2)	120 m
Breath (B_2)	14 m
Draft (D_2)	4.5 m
Centre of gravity	(0 m, 0 m, -0.5 m)
Displacement (V_D)	7,773 m^3
Roll inertia moment (I_{xx})	2.35×10^8 kg·m^2
Pitch inertia moment (I_{yy})	1.04×10^{10} kg·m^2
Yaw inertia moment (I_{zz})	1.17×10^{10} kg·m^2

The properties of the hawsers are summarized in Table 1 and the mooring configuration is shown in Table 4.

Table 3 Properties of the hawser lines

	Diameter	Density	EA	Length
Hawser1	0.052 m	10.3 kg/m	3120 kN	28.8 m
Hawser2				16.8 m
Hawser3				28.8 m
Hawser4				28.8 m
Hawser5				16.8 m
Hawser6				28.8 m

Table 4 Configuration of the hawser system

	Fairlead	Anchor
Hawser1	(50 m, 7 m 2 m)	(74 m, 24 m 1 m)
Hawser2	(50 m, 7 m 2 m)	(50 m, 24 m 1 m)
Hawser3	(50 m, 7 m 2 m)	(26 m, 24 m 1 m)
Hawser4	(-50 m, 7 m 2 m)	(-26 m, 24 m 1 m)
Hawser5	(-50 m, 7 m 2 m)	(-50 m, 24 m 1 m)
Hawser6	(-50 m, 7 m 2 m)	(-74 m, 24 m 1 m)

The hybrid numerical model used in the present simulation is based on the combination of the 3-D Rankine source method (Yuan et al., 2014) and the impulse response theory (Cummins, 1962). The 3-D Rankine source method is used to address the wash waves and the corresponding impact loads. Subsequently, the time-domain transient response of the moored ship subject to the wash waves is captured using the impulse response theory.

2.1 3-D RANKINE SOURCE METHOD

Assuming that the fluid is ideal, the velocity potential is used to describe the flow at any point within the fluid domain. It is well-known that the velocity potential satisfies the Laplace equation in the fluid domain, and therefore the calculation of the velocity potential is handled as the boundary value problem.

The potential φ_s of the wash wave is dealt with in the body-fixed coordinate system O_0-$X_0Y_0Z_0$ that moves together with the passing ship.

$$\begin{aligned}
&\nabla^2\varphi_s = 0, \text{in the fluid domain}\\
&\frac{\partial\varphi_s}{\partial \boldsymbol{n}} = Vn_1, \text{ on the passing ship}\\
&\frac{\partial\varphi_s}{\partial \boldsymbol{n}} = 0, \text{ on the moored ship}\\
&V^2\frac{\partial^2\varphi_s}{\partial x^2} + g\frac{\partial\varphi_s}{\partial z} = 0, \text{ on } z_0 = 0\\
&\frac{\partial\varphi_s}{\partial \boldsymbol{n}} = 0, \text{ on the harbour bank}
\end{aligned} \tag{1}$$

where $\boldsymbol{n} = (n_1, n_2, n_3)$ is the unit normal vector inward on the ship body surface. Once the wash wave potential φ_s is obtained, the wash wave impact loads acting on the moored ship are given by

$$\begin{aligned}
&F_i = \iint_S pn_i dS\\
&p = -\rho\left(\frac{\partial\varphi_s}{\partial t} - V\frac{\partial\varphi_s}{\partial x}\right)
\end{aligned}, \ i = 1, 2, \ldots, 6 \tag{2}$$

in which ρ is the water density and S is the wetted surface of the moored ship. The generalized normal vector n_i is defined as

$$n_i = \begin{cases} \boldsymbol{n}, i = 1,2,3 \\ \boldsymbol{r}\times\boldsymbol{n}, i = 4,5,6 \end{cases} \tag{3}$$

where $\boldsymbol{r} = (x, y, z)$ is the position vector.

In principle, it is required that the Rankine source should be distributed exactly on the undisturbed free surface. Nevertheless, a desingularized method is commonly used which raises the elements on the free water surface a short distance upwards (see Figure 2) (Zhang et al., 2010b). Meanwhile, the collocation points, where the boundary condition is satisfied, still stay exactly on the calm free surface. A raised distance $\nabla z = \sqrt{S}$ suggested by Zhang et al. (2010a) is selected, where S is the local element area.

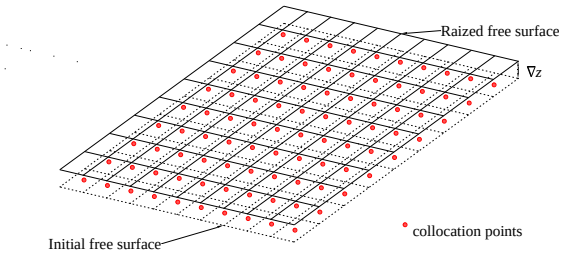

Figure 2. Raise of the free surface.

According to the description, the boundary of the fluid domain keeps varying during the passing process, requiring an update of the free surface truncation at each time step and the boundary value problem should be solved alongside with the update of the mesh distribution on the free surface. A re-meshing algorithm based on the concepts of the local mesh and the global mesh is developed. The local mesh is body-fixed and moves with the ship throughout the passing process. Comparatively, the global mesh can be understood as a kind of background mesh, which is fixed to the selected coordinate system. The essential idea of the re-meshing algorithm is to use the local mesh to overlap the global mesh and the complicated re-meshing problem will be converted in this way to a simple connection operation.

2.2 IMPULSE RESPONSE THEORY

According to the impulse response theory (Cummins, 1962), the time-domain motion equation of a floating body is given by

$$\sum_{j=1}^{6}\left[\left(M_{ij}+\mu_{ij}(\infty)\right)\ddot{x}_j(t)+\int_0^t h_{ij}(t-\tau)\dot{x}_j(t)d\tau+C_{ij}x_j(t)\right]=f_i(t)$$
$$i=1,2,...,6 \tag{4}$$

where M is the mass matrix, $\mu(\infty)$ is the added mass matrix at infinite frequency, $x(t)$, $\dot{x}(t)$ and $\ddot{x}(t)$ are the motion, the velocity and the acceleration, C is the static restoring stiffness matrix, $h_{ij}(t)$ is known as the retardation function, which can be represented by either the added mass or the radiation damping. $f_i(t)$ are the resultant external forces, including the wash wave impact loads and the hawser-fender tension forces. The wash wave impact loads are addressed with the 3-D Rankine source method (Eq. (2)).

The fender is simulated numerically with a linear-spring model, which is assumed to possess restoring stiffness on sway and roll modes merely. The restoring stiffness matrix of the fender is given by

$$K=\begin{bmatrix}0&0&0&0&0&0\\0&k&0&0&0&0\\0&0&0&0&0&0\\0&0&0&-k\cdot L&0&0\\0&0&0&0&0&0\\0&0&0&0&0&0\end{bmatrix} \tag{5}$$

where k = 3800 kN is the stiffness of the fender. L is the lever arm. Considering that the fender is 0.5 m above the centre of gravity of the moored ship, L = 0.5 m is used in the present research.

The hawser is simulated with the lumped-mass approach. As shown in Figure 3, the hawser is divided into a series of evenly-sized segments, which are represented by connected nodes and spring and damper systems. Please refer to (Hall and Goupee, 2015) for more details of the model.

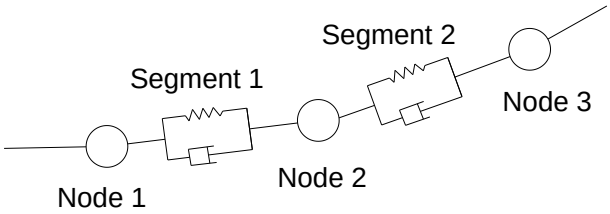

Figure 3. Lumped-mass model of the hawser.

3 VALIDATION

The simulation results given by Janson et al. (2003) are used here to check whether the present simulation tool is able to capture the wash wave pattern. A combined Rankine/Kelvin source method was developed by Janson et al. (2003), where the near-field and far-field wash waves were computed by the higher-order Rankine source and the Kelvin source, respectively. Figure 4 shows the far-field wash wave elevation η produced by a sailing Wigley ship in open calm water with forward speed Fr = 0.316. Considering that the far-field wash wave was calculated with the Kelvin source in (Janson et al., 2003) whereas the present model uses the linear Rankine source, the agreement is acceptable.

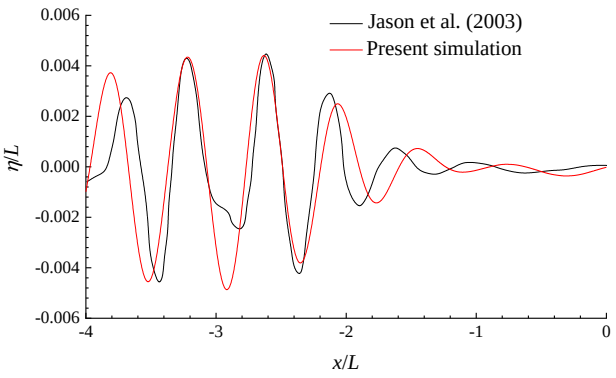

Figure 4. Validation of wash wave cut at $y = 0.75L$, $Fr = 0.316$.

4 SIMULATION RESULTS

4.1 TRANSIENT RESPONSES

Figure 5 displays the wash wave pattern throughout the passing process in calm water. The Froude number *Fr* is 0.8. The lateral separation between the two ships is 40 m. When the wash waves reach the port bank, they are reflected and propagate back to the transverse wave region. On the contrary, the wash waves on the other side are free to propagate outward. Three stages are identified during the passing process. In the first stage, the Kelvin wave has not arrived the moored ship yet, so that the near-field water surface around the moored ship is still. As the passing ship continues advancing ahead, the moored ship enters the divergent wave region. It can be seen that the divergent wash waves are reflected at the starboard of the moored ship, implying that the moored ship is subject to the wash wave impact load. Finally, the divergent wave region passes by the ship in which stage the ship is surrounded by the transverse waves and the reflected divergent waves.

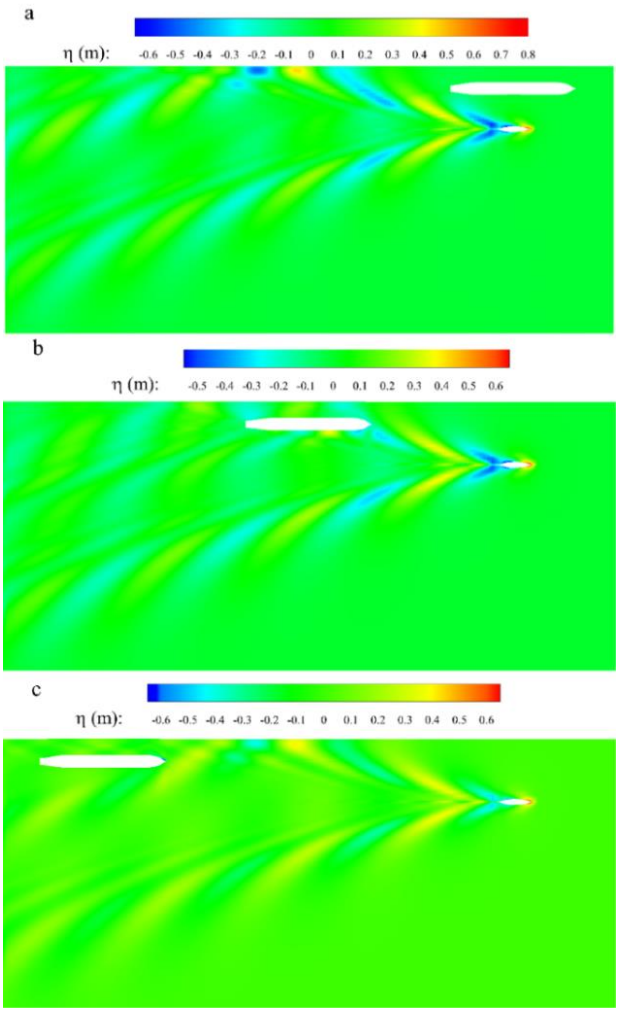

Figure 5. Wash wave patterns (displayed in the body-fixed coordinate system), *Fr* = 0.8, B_S = 40 m. (a) Stage 1; (b) Stage 2; (c) Stage 3.

Figure 6 plots the transient motions of the moored ship induced by the wash waves alone. When the wash waves reach, the moored ship is subject to the impact load immediately and strong response is induced in a short time. Afterward, the ship decays gradually since the wash wave region has overtaken the moored ship. Therefore, decay-type responses are observed during the process. Due to the pre-tension of the hawsers, the mean positions of sway and roll are non-zero.

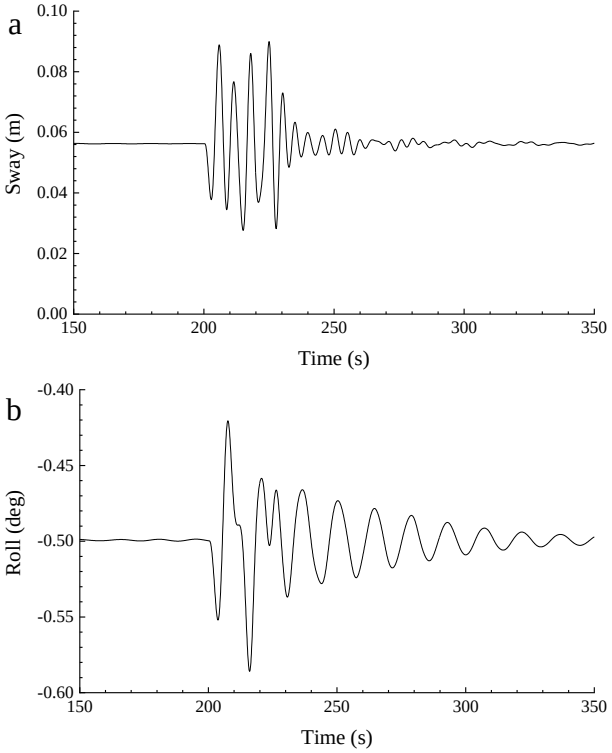

Figure 6. Time series of ship motions, *Fr* = 0.8, B_S = 40 m. (a) sway motion; (b) roll motion.

The transient effect is also observed in the fender compression force. As shown in Figure 7, the compression force is initially stable at 215 kN to resist the pre-tension of the hawsers. During the transient stage, the fender also experiences a decay-type response and returns to the initial state finally. A similar phenomenon is also observed in the hawser force as displayed in Figure 8.

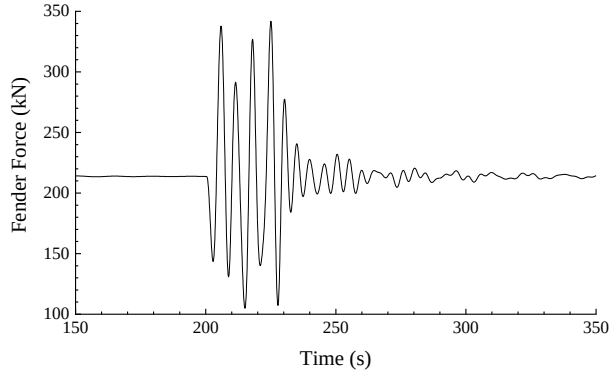

Figure 7. Time series of fender compression, *Fr* = 0.8, B_S = 40 m.

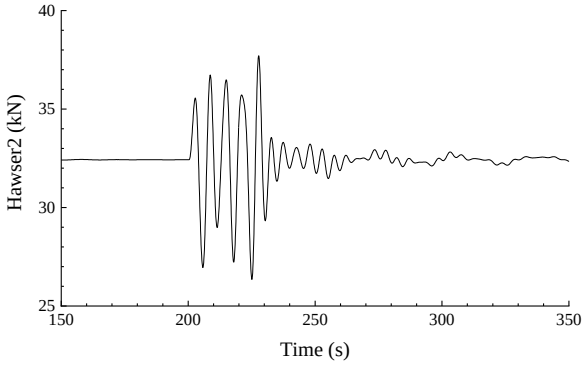

Figure 8. Time series of hawser force (hawser 2), *Fr* = 0.8, B_S = 40 m.

4.2 EFFECT OF FORWARD SPEED

The ship motions with different passing ship's forward speeds are compared in Figure 9 (The lateral distance is fixed at 40 m). As the forward speed of the passing ship drops, the transient ship motions reduce accordingly. The maximum amplitude of heave motion is 0.048 m when *Fr* = 0.8. This value drops to as low as 0.01 m if *Fr* reduces to 0.5. It is straightforward to understand such a variation trend as the wash wave elevation drops if the forward speed becomes smaller. The divergent wash waves are very limited for low Froude number condition, in which case the energy is mainly carried by the transverse waves.

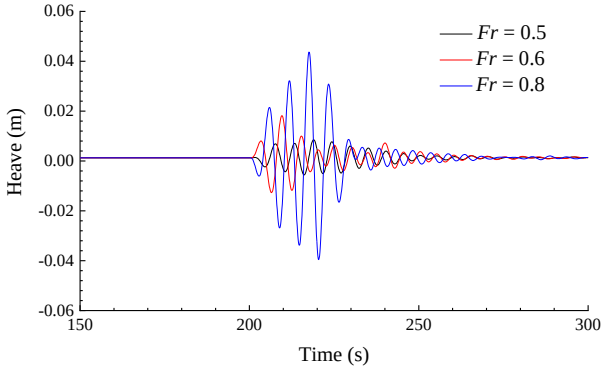

Figure 9. Times series of ship heave motion at different forward speeds, B_S = 40 m.

A similar variation trend is seen in the fender force and the hawser force, which is displayed in Figure 10 and Figure 11, respectively.

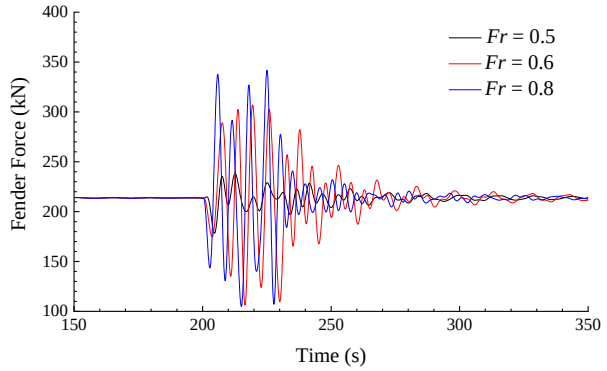

Figure 10. Time series of fender compression at different forward speeds, B_S = 40 m.

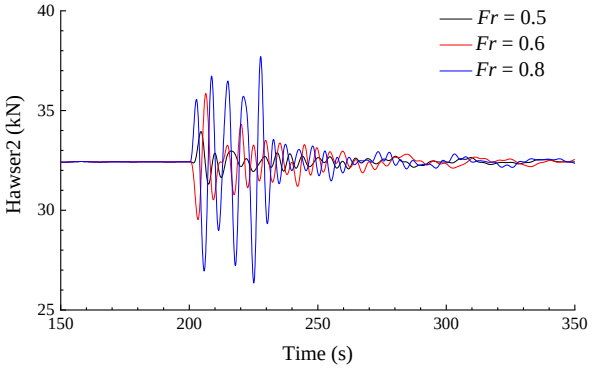

Figure 11. Time series of hawser force (hawser 2) at different forward speeds, B_S = 40 m.

4.3 EFFECT OF DISTANCE

The influence of the wash waves propagation distance on the transient response is investigated by increasing the lateral distance from 40 m to 60 m so that the wash waves will travel another 20 m to reach the moored ship (The Froude number is fixed at 0.8). Figure 12 displays the transient ship motions with different propagation distances. The fender forces are shown in Figure 13. As shown, the characteristics of the two curves are very similar. It seems that the propagation of the wash waves has a tiny influence on the ship transient motions.

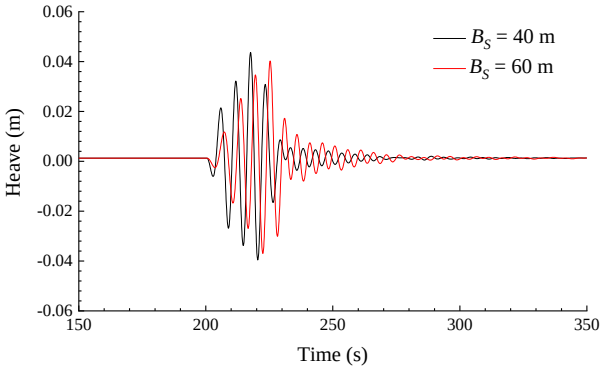

Figure 12. Time series of ship motions with various lateral distances, B_S = 0.8.

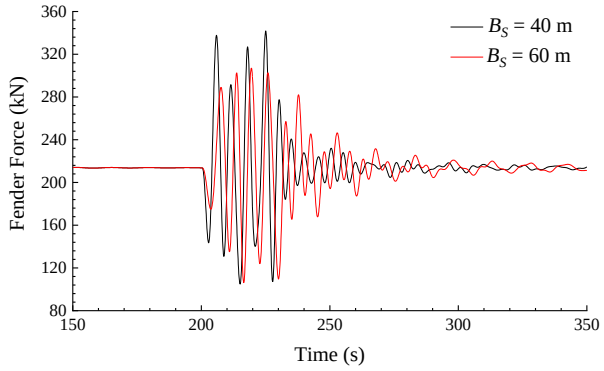

Figure 13. Time series of fender force with various lateral distances, B_S = 0.8.

The propagation distance effect on the transient response is tiny, since the divergent wash waves dissipate little

during the propagation process. Figure 14 compares the wash wave patterns and Figure 15 shows the near-field wave elevation at the starboard of the moored ship (along the black line in Figure 14), when the divergent waves just arrive the bow of the moored ship. It is shown that the wave patterns are similar and the divergent waves dissipate hardly even if they travel a longer distance. Therefore, the transient responses in the two cases are similar to each other.

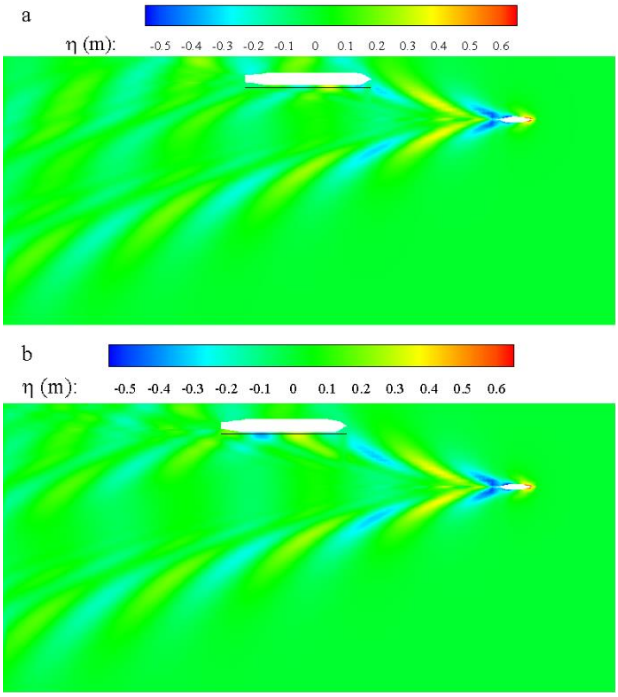

Figure 14. Wash wave pattern with different propagation distances (displayed in the body-fixed coordinate system), *Fr* = 0.8. (a) B_S = 40 m; (b) B_S = 60 m.

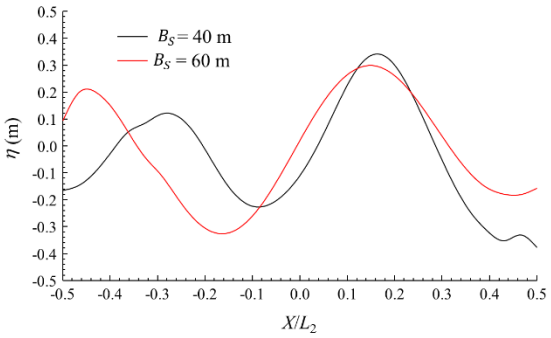

Figure 15. Near-field wave elevation at the starboard of the moored ship, *Fr* = 0.8.

5 CONCLUSIONS

A hybrid numerical model based on the 3-D Rankine source method and the impulse response theory is developed to address the transient response of a moored ship under the wash waves produced a passing ship. The wave-structure interaction is firstly simulated with the 3-D Rankine source method. Afterwards, a time-domain analysis is performed to simulate the transient response of the moored ship.

The moored ship is subjected to significant wash wave impact loads even if the passing ship is travelling far away. The transient effect is observed in the ship motions and the mooring line tensions. A decay-type response is observed during the transient duration.

The propagation distance of the wash waves seems to have little influence on the transient response. The transient response is sensitive to the ship speed. A fast passing ship induces strong transient response of the moored ship.

6 REFERENCES

Cummins, W., 1962. The impulse response function and ship motions. David Taylor Model Basin, Washington DC, pp. 101-109.

Hall, M., Goupee, A., 2015. Validation of a lumped-mass mooring line model with DeepCwind semisubmersible model test data. Ocean Engineering 104, 590-603. https://doi.org/10.1016/j.oceaneng.2015.05.035

Janson, C.E., Leer-Andersen, M., Larsson, L., 2003. Calculation of deep-water wash waves using a combined Rankine/Kelvin source method. Journal of Ship Research 47 (4), 313-326.

Jiang, T., Henn, R., Sharma, S.D., 2002. Wash waves generated by ships moving on fairways of varying topography, in: Proceedings of the 24th Symposium on Naval Hydrodynamics, Fukuoka, Japan, pp. 441-457.

Li, L., Yuan, Z.-M., Ji, C., Li, M.-X., Gao, Y., 2018a. Investigation on the unsteady hydrodynamic loads of ship passing by bridge piers by a 3-D boundary element method. Engineering Analysis with Boundary Elements 94 (C), 122-133. https://doi.org/10.1016/j.enganabound.2018.06.010

Li, L., Yuan, Z.M., Gao, Y., 2018b. Wash wave effects on ships moored in ports. Applied Ocean Research 77, 89-105. https://doi.org/10.1016/j.apor.2018.06.001

Pinkster, J., Naaijen, P., 2003. Predicting the effect of passing ships, in: Proceedings of the 18th Int. Workshop on Water Waves and Floating Bodies. Le Croisic, France.

Pinkster, J.A., 2009. Suction, Seiche and Wash Effects of Passing Ships in Ports, in: Proceedings of the Annual Meeting of the Society of Naval Architects and Marine Engineers (SNAME), Providence.

van der Molen, W., Wenneker, I., 2008. Time-domain calculation of moored ship motions in nonlinear waves. Coastal Engineering 55 (5), 409-422. https://doi.org/10.1016/j.coastaleng.2008.01.001

Vantorre, M., Verzhbitskaya, E., Laforce, E., 2002. Model test based formulations of ship-ship interaction forces. Ship Technology Research 49, 124-141.

Yuan, Z.M., Incecik, A., Alexander, D., 2014. Verification of a new radiation condition for two ships

advancing in waves. Applied Ocean Research 48, 186-201.
https://doi.org/10.1016/j.apor.2014.08.007

Zhang, X.S., Bandyk, P., Beck, R.F., 2010a. Seakeeping computations using double-body basis flows. Applied Ocean Research 32 (4), 471-482.
https://doi.org/10.1016/j.apor.2010.10.003

Zhang, X.S., Bandyk, P., Beck, R.F., 2010b. Time-Domain Simulations of Radiation and Diffraction Forces. Journal of Ship Research 54 (2), 79-94.

Janson, C.E., Leer-Andersen, M., Larsson, L., 2003. Calculation of deep-water wash waves using a combined Rankine/Kelvin source method. Journal of Ship Research 47 (4), 313-326.

Jiang, T., Henn, R., Sharma, S.D., 2002. Wash waves generated by ships moving on fairways of varying topography, 24th Symposium on Naval Hydrodynamics, Fukuoka, Japan, pp. 441-457.

Li, L., Yuan, Z.M., Gao, Y., 2018a. Wash wave effects on ships moored in ports. Applied Ocean Research 77, 89-105.
https://doi.org/10.1016/j.apor.2018.06.001

Li, L., Yuan, Z.M., Ji, C.Y., Li, M.X., Gao, Y., 2018b. Investigation on the unsteady hydrodynamic loads of ship passing by bridge piers by a 3-D boundary element method. Engineering Analysis with Boundary Elements 94 (C), 122-133.
https://doi.org/10.1016/j.enganabound.2018.06.010

Pinkster, J., Naaijen, P., 2003. Predicting the effect of passing ships, Proc. 18th Int. Workshop on Water Waves and Floating Bodies. Le Croisic, France.

Pinkster, J.A., 2009. prop, Proceedings of the Annual Meeting of the Society of Naval Architects and Marine Engineers (SNAME), Providence,, p. 99.

van der Molen, W., Wenneker, I., 2008. Time-domain calculation of moored ship motions in nonlinear waves. Coastal Engineering 55 (5), 409-422.
https://doi.org/10.1016/j.coastaleng.2008.01.001

Vantorre, M., Verzhbitskaya, E., Laforce, E., 2002. Model test based formulations of ship-ship interaction forces. Ship Technology Research 49, 124-141.

Yuan, Z.M., Incecik, A., Alexander, D., 2014. Verification of a new radiation condition for two ships advancing in waves. Applied Ocean Research 48, 186-201.
https://doi.org/10.1016/j.apor.2014.08.007

Zhang, X.S., Bandyk, P., Beck, R.F., 2010a. Seakeeping computations using double-body basis flows. Applied Ocean Research 32 (4), 471-482.
https://doi.org/10.1016/j.apor.2010.10.003

Zhang, X.S., Bandyk, P., Beck, R.F., 2010b. Time-Domain Simulations of Radiation and Diffraction Forces. Journal of Ship Research 54 (2), 79-94.

7 AUTHORS BIOGRAPHY

Liang Li holds the current position of Research Associate at University of Strathclyde. His previous experience includes ship hydrodynamics, offshore renewable energy and energy control.

Zhi-Ming Yuan holds the current position of Lecturer at University of Strathclyde. His previous experience includes ship hydrodynamics, multi-body hydrodynamic interactions.